Heliyon 9 (2023) e16578

Contents lists available at ScienceDirect

Heliyon

journal homepage: www.cell.com/heliyon

Research article

# Unsteady hybrid nanofluid (Cu-UO2/blood) with chemical reaction and non-linear thermal radiation through convective boundaries: An application to bio-medicine

Mubashir Qayyum [a], Sidra Afzal [a], Syed Tauseef Saeed [a], Ali Akgül [b,c,d], Muhammad Bilal Riaz [e,f,g,*]

[a] Department of Sciences and Humanities, National University of Computer and Emerging Sciences, Lahore, Pakistan
[b] Siirt University, Art and Science Faculty, Department of Mathematics, 56100 Siirt, Turkey
[c] Near East University, Mathematics Research Center, Department of Mathematics, Near East Boulenvard, PC:99138 Nicosia/Mersin 10, Turkey
[d] Department of Computer Science and Mathematics, Lebanese American University, Beirut, Lebanon
[e] Faculty of Technical Physics, Information Technology and Applied Mathematics, Lodz University of Technology, 90-924 Lodz, Poland
[f] Department of Computer Science and Mathematics, Lebanese American University, Byblos, Lebanon
[g] Department of Mathematics, University of Management and Technology, 54770 Lahore, Pakistan

ARTICLE INFO

*Keywords:*
Hybrid nanofluid
Blood flow
Non-linear thermal radiation
Chemical reaction
Convective boundary conditions
Optimal q-homotopy analysis method

ABSTRACT

This study is focused on modeling and simulations of hybrid nanofluid flow. Uranium dioxide $UO_2$ nanoparticles are hybrid with copper $Cu$, copper oxide $CuO$ and aluminum oxide $Al_2O_3$ while considering blood as a base fluid. The blood flow is initially modeled considering magnetic effect, non-linear thermal radiation and chemical reactions along with convective boundaries. Then for finding solution of the obtained highly nonlinear coupled system we propose a methodology in which q-homotopy analysis method is hybrid with Galerkin and least square Optimizers. Residual errors are also computed in this study to confirm the validity of results. Analysis reveals that rate of heat transfer in arteries increases up to 13.52 Percent with an increase in volume fraction of $Cu$ while keeping volume fraction of $UO_2$ fixed to 1% in a base fluid (blood). This observation is in excellent agreement with experimental result. Furthermore, comparative graphical study of $Cu$, $CuO$ and $Al_2O_3$ for increasing volume fraction is also performed keeping $UO_2$ volume fraction fixed. Investigation indicates that $Cu$ has the highest rate of heat transfer in blood when compared with $CuO$ and $Al_2O_3$. It is also observed that thermal radiation increases the heat transfer rate in the current study. Furthermore, chemical reaction decreases rate of mass transfer in hybrid blood nanoflow. This study will help medical practitioners to minimize the adverse effects of $UO_2$ by introducing hybrid nano particles in blood based fluids.

## 1. Introduction

Nanofluids have gathered much interest from researchers as they play a pivotal role in enhancing thermal transport in fluids by including suitable nano-scaled particles to a fluid. This will alter many physical properties. Primarily, the idea of adding particles of

* Corresponding author.
*E-mail address:* muhammad.riaz@p.lodz.pl (M.B. Riaz).

https://doi.org/10.1016/j.heliyon.2023.e16578
Received 10 December 2022; Received in revised form 19 May 2023; Accepted 20 May 2023
Available online 26 May 2023
2405-8440/

**Nomenclature**

Parameters with units

| | | |
|---|---|---|
| $r, \vartheta, z$ | radial, axial and tangential coordinates $t$ temporal coordinate | (s) |
| $u, v, w$ | velocity along $r, \vartheta, z$ axis | ($ms^{-1}$) |
| $\nu_{hnf}$ | kinematic viscosity | ($m^2s^{-1}$) |
| $\sigma_{hnf}$ | electric conductivity | ($Sm^{-1}$) |
| $B_0^2$ | magnetic field strength | ($Am^{-1}$) |
| $\rho_{hnf}$ | density | ($kgm^{-3}$) |
| $(\rho C_p)_{hnf}$ | specific heat | (J/kgK) |
| $D_{hnf}$ | thermal diffusivity | ($m^2s^{-1}$) |
| $k_r^2$ | chemical reaction rate | ($Ms^{-1}$) |
| $\tilde{E}$ | activation energy | ($JM^{-1}$) |
| $k$ | thermal conductivity | (W/mK) |
| $T$ | temperature | (K) |
| $C$ | concentration | ($kgm^{-3}$) |
| $a_1, a_2$ | stretching rates | ($s^{-1}$) |
| $\omega$ | angular frequency | ($s^{-1}$) |
| $b$ | positive constant | ($s^{-1}$) |
| $h_1, h_2$ | heat transfer coefficients | |

Dimensionless parameters

| | |
|---|---|
| $\eta$ | independent variable |
| $F', G, F$ | radial, tangential and axial velocities |
| $\theta, \phi$ | temperature, concentration |
| $Et$ | activation energy parameter |
| $\tilde{A}_1, \tilde{A}_2$ | stretching parameters |
| $\wp_i, T_w$ | nanofluid parameters, temperature ratio |
| $B, R^*$ | unsteady parameter, radiation parameter |
| $Pr, Sc$ | Prandtl number, Schmidt number |
| $M, W_s$ | magnetic parameter, suction parameter |
| $\mathbb{B}_1, \mathbb{B}_2$ | Biot numbers |
| $\sigma_t$ | chemical reaction rate |
| $\delta_1, Re$ | temperature difference, Reynolds number |

Subscripts

| | |
|---|---|
| $hnf$ | hybrid nanofluid |
| $bf$ | base fluid |
| $UO_2$ | uranium dioxide |
| $Cu, CuO$ | copper, copper oxide |
| $Al_2O_3$ | aluminum oxide |

micro-size to coolants was presented by Maxwell [1] in 1904 but it was not a success due to some set backs to the study. This idea caught attention again in 1995 when Choi [2] first introduced the term “nanofluid”. In general, nanofluid contains nanometer sized particles named as nanoparticles. Mostly carbides, oxides or metals are taken as nanoparticles and common base fluids are ethylene glycol, water, blood or oils. Afterwards, nanofluid caught the limelight for over the past two decades and researchers have introduced many combinations of these nanofluids to analyze and optimize the heat transfer and other physical phenomena analytically as well as experimentally. Turkyilmazoglu [3] studied heat transfer of a nanofluid on a rotating disk. Highest shear rate in this case was offered by silver nanoparticles. Magnetic effects on nanofluid heat transfer between two plates was investigated by Sheikholeslami et al. [4]. Huminic and Huminic [5] analyzed entropy generation in nanofluid in various kinds of thermal systems. Study on $CuO$-water nanofluids in microchannels was done by Li and Kleinstreuer [6]. Ghalandari et al. [7] simulated nanofluid flow to optimize root canal procedures and efficient removal of microorganisms. Sheikholeslami et al. [8] also scrutinized a two-phase model of nanofluids influenced by thermal radiations and magneto-hydrodynamic effects. Raza et al. [9] analyzed a water based Casson fluid model impacted by inclined magnetic forces. Qayyum et al. [10] presented a study on squeezing flow of a water-based nanofluid in three dimensions in a rotating channel. Alharbi et al. [11] studied the effects of single and multi-walled nanotubes on water and blood based nanofluids comparatively on an inclined surface with slip conditions. Flow of a second grade nanofluid with Catteno-Christov heat flux is simulated by Gangadhar et al. [12]. Zohra et al. [13] analyzed the Buongiorno model of Casson nanofluid with Navier slip boundaries flowing inside a stretchable channel. Many researchers scrutinized nanofluid flow problems with different geometries under various physical effects [14–21].

Extending the scope of nanofluids, hybrid nanofluids were formerly introduced by Suresh et al. [22] in 2012. The basic idea of hybrid nanofluid is to add two different nano-meter sized particles in a base-fluid in order to enhance the heat transfer properties of the newly developed hybrid nanofluid. Suresh et al. combined $Al_2O_3$ and $Cu$ nanocomposite in water and thoroughly investigated the hybrid nanofluid properties experimentally which were then compared with empirical results as well. It was deduced from the study that heat transfer rate was enhanced up to 13.5% as compared to water and was also greater than two-phase nanofluid $Al_2O_3$-water. There results were in good agreement with empirical results of the study pointing out the significance and validity of empirical analysis on hybrid nanoflows. As much as these fluids are important in engineering, they also have vast implications in medical sciences. Many drugs are produced in form of hybrid nanofluids and in order to study the chemical reactive behavior on human body, blood is taken as test base-fluid. In case of normal circulation through arteries a sustainable temperature and blood transmission is required through human body. Thermal properties of blood are required to be enhanced in various physical conditions through hybridization of blood with various nanoparticles. According to the nature of nanofluids they are important in pollution purification purpose, pharmaceutical nanoliquids and drug delivery through arteries. Alghamdi et al. [23] analyzed hybrid nanofluid flow under magnetohydrodynamic effect. They studied blood based fluid with $Cu$ and $CuO$ nanoparticles between two permeable channels. There findings supported more effective thermal analysis in case of $Cu$-$CuO$/blood fluid in comparison with $Cu$/blood fluid. On similar pattern, Dinarvand et al. [24] investigated $Cu$-$CuO$/blood hybrid nano-flow under mixed convection and MHD effect over a porous and stretching sheet. They used bvp4c built-in routine to solve the system of governing equations. This study showed that blade shape of both nanoparticles enhanced rate of heat transfer indefinitely. Shahazadi and Bilal [25] recently simulated bifurcated stenosed artery model to enhance drug delivery with help of hybrid nanofluid having blood as base-fluid. Permeability was considered in walls of stenosed artery with copper and copper oxide used as nanoparticles in blood for enhancing drug transport.

Abdelsalam et al. [26] empirically analyzed aneurysmal/stenosed segment of a diseased artery usinh hybrid blood nanofluid flow. It was observed that velocity of blood decreased the most incase of spherically shaped nanoparticles when compared with platelet, rods and bricks shaped nanoparticles in hybrid flow. Chahregh and Dinarvand [27] also studied blood-hybrid nanofluid but they used $TiO_2$ and $Ag$ as nanoparticles passing through a porous channel. Both walls of channel were considered at different permeability which allowed the fluid flow with dilation and squeezing of the walls. The analysis that varying permeability caused asymmetry to the flow channel resulting in significant change on th blood flow. Alsharif et al. [28] enhanced a micro-pump performance with help of second grade hybrid nanofluid with copper and titanium nanoparticles. Shah et al. [29] optimized entropy in flow of a hybrid nanofluid on a curved surface. Alhowaity et al. [30] studied flow of a hybrid nanofluid passing over a moving sheet with non-Fourier energy transmission. Wang et al. [31] analyzed hybrid nanofluid flow passing through a porous medium with heat sink. Madhukesh et al. [32] performed simulations on a water based hybrid nanofluid passing on a curved stretching sheet with special effects of non-Fourier heat flux.

Human blood contains erythrocyte cells which adds the magnetic factor in blood flow through arterial walls. Iftikhar et al. [33] studied peristaltic blood flow through an endoscopic non-uniform tube with gold nanoparticles. Cylindrical, spherical and blade shaped nanoparticles are considered comparatively. Gandhi et al. [34] optimized entropy of the $Au$-$Al_2O_3$/blood hybrid nanofluid with MHD effect, viscous dissipation and Joule heating. As a result, it was noted that entropy increased with increase in shape factor of both nanoparticles within the stenotic zone of the artery. Kumar et al. [35] investigated MHD blood flow in bifurcated arteries under impact of chemical reaction. MHD effect with blood flow has been studied by many authors in literature. Khalid et al. [36] studied MHD blood flows with CNT nanoparticles passing through a porous channel. Peristaltic wave flow of blood was analyzed by Rashidi et al. [37] with effect of MHD. Rashidi et al. [38] also investigated MHD blood flow through Casson fluid model. Wang et al. [39] simulated shear thinning and thickening profiles of blood based hybrid Casson nanofluid under effect of a constant magnetic field. Elogail and Mekheimer [40] studied flow of blood passing through a microvessel that involved oxytactic microorganisms along with nanoparticles. Bingham nanofluid blood flow problem with MHD effect nd hom-het reactions is analyzed by Tanveer et al. [41]. Gangadhar et al. [42] presented a hydrothermal analysis on graphene and ferrous oxide hybrid nanofluid in a magnetized rotating cylinder. Bhatti and Abbas [43] modeled peristaltic blood flow problem with Jeffrey fluid under combined effect of slip parameters and MHD which is applicable in drug targeting during cancer. Blood flow through bifurcated arteries under effects of MHD and heat source is simulated by Prakash et al. [44].

In medical sciences, the biological systems undergo many reactions biochemically and mediated through various enzymes in the body. Chemical reaction effects are significant in study of blood flow and scrutinized by researcher through both in-vivo and in-vitro analysis. Tripathi and Sharma [45] studied pulsatic flow of blood passing though an artery that was stenosed. Chemical reaction effects were also highlighted in this study. It was deduced that two-phase model of blood flow was more accurate when compared with single-phase blood flow model of the nanofluid. Roy and Beg [46] recently studied a blood flow problem with bulk reaction for both micropolar and Newtonian fluid. Closed form solutions are developed and hemodynamic properties of blood flow are investigated. Blood concentration was increased as reaction rate elevated. Ellahi et al. [47] studied peristaltic flow of blood with gold nanoparticles in presence of activation energy and chemical reaction. Basha and Sivaraj [48] studied blood nanofluid having gyrotactic microorganisms and chemical reactions with three different geometries. Okuyade et al. [49] analyzed blood flow in merging veins with chemical reactions influencing blood flow. Rasool and Zhang [50] studied Powell-Eyring nanofluid flow on a radiative riga plate with convective boundary conditions and chemical reaction. Entropy generation of a Casson nanofluid impacted by activation energy flowing on a non-linearly stretched surface was investigated by Shah et al. [51]. Khan et al. [52] performed second law analysis on a nanofluid impacted by Arrhenius activation energy.

In light of literature review stated above, the authors of this study noticed a research gap on unsteady hybrid blood nanofluid flow with two type of nanoparticles, uranium dioxide and copper/copper oxide/aluminum oxide and to enhance the heat and mass transfer effects. This study will be useful for medical practitioners to reduce the adverse effects of uranium on blood stream by introducing various nanoparticles on a blood based hybrid nanofluid. In this study, the blood flow through arteries is modeled with impact of chemical reaction, magnetohydrodynamic effect, non-linear thermal radiation and thermally convective boundaries. The developed flow problem is a mathematical depiction of blood flow through arterial walls. Moreover, skin friction, Nusselt and Sherwood number for current flow geometry are also investigated. In order to solve the obtained system of non-linear problems a new algorithm optimal q-homotopy analysis method is utilized [53–55]. Optimal values of convergence control parameters are calculated through least square and Galerkin's method. Furthermore, average squared residual errors are computed for validation purpose. Conclusions are drawn through simulations of blood velocity, temperature, concentration, skin friction with arterial walls, heat and mass transfer for various volume fractions and different nanoparticles. Section 2 shows modeling of the flow problem, Section 3 depicts basic methodology of the used method, analysis on convergence of the problem is done in Section 4, discussion on obtained results is in Section 5 and finally conclusions of the current study are drawn in Section 6.

## 2. Model formulation

We consider flow problem of blood through arteries with various physical effect influencing the blood flow. In this regard, a hybrid nanofluid flow is modeled with axially symmetric flow in cylindrical coordinates $(r, \vartheta, z)$. Flow geometry of the test problem is shown in Fig. 1. The blood flow is influenced by MHD (with induced magnetic field $B_0$ acting in perpendicular direction), non-linear thermal radiation, chemical reaction with activation energy and thermally convective boundary conditions. Governing equations of the flow problem are devised as follows:

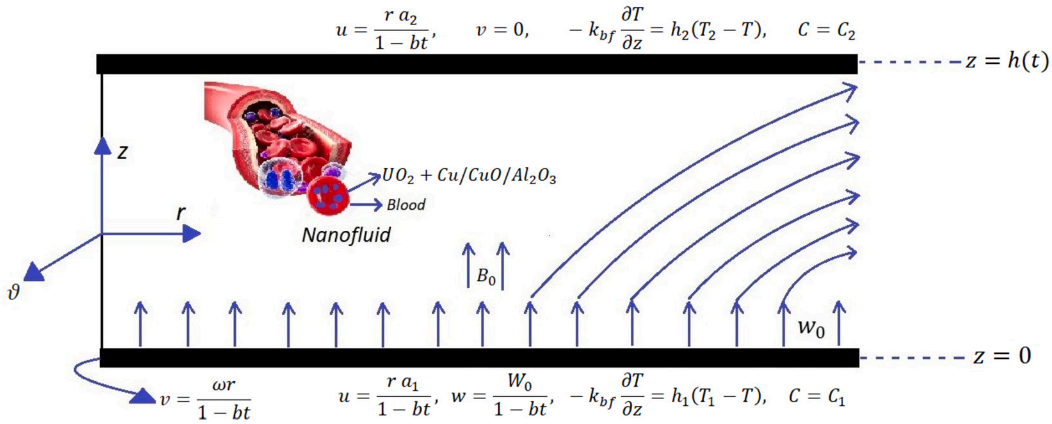


**Fig. 1.** Blood flow geometry.

$$u_r + \frac{u}{r} + w_z = 0, \tag{1}$$

$$u_t + uu_r + wu_z - \frac{v^2}{r} = \nu_{hnf}\nabla^2 u - \frac{\sigma_{hnf}B_0^2}{\rho_{hnf}}u, \tag{2}$$

$$v_t + uv_r + wv_z + \frac{uv}{r} = \nu_{hnf}\nabla^2 v - \frac{\sigma_{hnf}B_0^2}{\rho_{hnf}}v, \tag{3}$$

$$T_t + uT_r + wT_z = \frac{k_{hnf}}{(\rho Cp)_{hnf}}\nabla^2 T + \frac{1}{(\rho Cp)_{hnf}}\frac{\partial q_r}{\partial z}, \tag{4}$$

$$C_t + uC_r + wC_z = D_{hnf}\frac{\partial^2 C}{\partial z^2} - k_r^2(C - C_2)\left(\frac{T}{T_2}\right)^m e^{\frac{-\tilde{E}}{k^* T}}, \tag{5}$$

subject to the following boundary conditions

$$\begin{aligned} &u = \frac{a_1 r}{1-bt}, \quad v = \frac{r\omega}{1-bt}, \quad w = \frac{W_0}{1-bt} \quad -k_{bf}\frac{\partial T}{\partial z} = h_1(T_1 - T), \quad C = C_1 \quad at \quad z = 0 \\ &u = \frac{a_2 r}{1-bt}, \quad v = 0, \quad -k_{bf}\frac{\partial T}{\partial z} = h_2(T_2 - T), \quad C = C_2 \quad at \quad z = h(t) = \sqrt{\frac{\nu(1-bt)}{\omega}} \end{aligned} \tag{6}$$

where velocity components in $r$, $\vartheta$ and $z$-direction are $u$, $v$ and $w$ respectively. T and C are the blood temperature and concentration. $B_0$ is the magnetic field applied in normal direction to $z = 0$, $k_r$ is the chemical reaction rate, $\tilde{E}$ is the energy to activate chemical reaction, $m$ is a constant power and $(q_r)_z$ the radiative non-linear heat flux is defined by Rosseland's approximation [56] as:

$$q_r = -\frac{4\tilde{\sigma}}{3\tilde{k}}(T^4)_z = -\frac{16\tilde{\sigma}}{3\tilde{k}}T^3(T)_z, \tag{7}$$

here, $\tilde{\sigma}$ is the Stefan-Boltzmann constant and $\tilde{k}$ is the coefficient of mean absorption. Stefan Boltzmann law states that all the objects possessing temperature greater than absolute zero emit radiations that are proportional to fourth power of their absolute temperature. Moreover, optically thick fluids are characterized through Rosseland's approximation. The non-linear temperature term $T^4$ is expanded through Taylor series expansion and by considering the temperature difference to be insignificant within the fluid flow. By using Eq. (7) in Eq. (4), temperature equation is finalized as follows:

$$T_t + uT_r + wT_z = \frac{k_{hnf}}{(\rho Cp)_{hnf}}\nabla^2 T + \frac{1}{(\rho Cp)_{hnf}}\frac{\partial}{\partial z}\left(\frac{16\tilde{\sigma}}{3\tilde{k}}T^3\frac{\partial T}{\partial z}\right). \tag{8}$$

Basic characteristics of hybrid nanofluid are given in Table 1. Here, $\nu_{hnf}$, $\rho_{hnf}$, $\sigma_{hnf}$, $k_{hnf}$, $(\rho Cp)_{hnf}$, $D_{hnf}$ are viscosity, density, electrical conductivity, thermal conductivity, heat capacitance and thermal diffusivity of hybrid nanofluid. Moreover, $'bf'$ corresponds to base fluid blood properties, $UO_2$ and $Cu/CuO/Al_2O_3$ are nanoparticle properties.

Following similarity transforms are introduced [58,59]

$$\begin{aligned} &u = \frac{\omega r}{1-bt}F'(\eta), \quad v = \frac{\omega r}{1-bt}G(\eta), \quad w = -2\sqrt{\frac{\omega\nu_{bf}}{1-bt}}F(\eta), \\ &\eta = z\sqrt{\frac{\omega}{\nu_{bf}(1-bt)}}, \quad \theta(\eta) = \frac{T - T_2}{T_1 - T_2}, \quad \phi(\eta) = \frac{C - C_2}{C_1 - C_2} \end{aligned} \tag{9}$$

By employing Eq. (9) in Eqs. (1)-(8) we obtain following ordinary differential equations of the flow geometry

**Table 1**
Thermophysical characteristics of hybrid nanofluid where $Cu$ can be replaced by $CuO$ and $Al_2O_3$ [57].

| Properties | Hybrid nanofluid |
|---|---|
| Volume fraction | $\varphi_{hnf} = \varphi_{UO_2} + \varphi_{Cu}$ |
| Kinematic viscosity | $\nu_{hnf} = \frac{\mu_{hnf}}{\rho_{hnf}}$ |
| Density | $\rho_{hnf} = (1-\varphi_{hnf})\rho_{bf} + \varphi_{Cu}\rho_{Cu} + \varphi_{UO_2}\rho_{UO_2}$ |
| Dynamic viscosity | $\mu_{hnf} = \frac{\mu_{bf}}{(1-\varphi_{Cu})^{5/2}(1-\varphi_{UO_2})^{5/2}}$ |
| Heat capacity | $(\rho Cp)_{hnf} = (1-\varphi_{hnf})(\rho Cp)_{bf} + \varphi_{Cu}(\rho Cp)_{Cu} + \varphi_{UO_2}(\rho Cp)_{UO_2}$ |
| Thermal conductivity | $\frac{k_{hnf}}{k_{bf}} = \frac{\varphi_k + 2k_{bf} + 2(\varphi_{Cu}k_{Cu} + \varphi_{UO_2}k_{UO_2}) - 2\varphi_{hnf}k_{bf}}{\varphi_k + 2k_{bf} - (\varphi_{Cu}k_{Cu} + \varphi_{UO_2}k_{UO_2}) + \varphi_{hnf}k_{bf}}$ where $\varphi_k = \frac{\varphi_{Cu}k_{Cu} + \varphi_{UO_2}k_{UO_2}}{\varphi_{hnf}}$ |
| Thermal diffusivity | $\frac{D_{hnf}}{D_{bf}} = (1-\varphi_{hnf})$ |
| Electrical conductivity | $\frac{\sigma_{hnf}}{\sigma_{bf}} = \frac{\varphi_\sigma + 2k_{bf} + 2(\varphi_{Cu}\sigma_{Cu} + \varphi_{UO_2}\sigma_{UO_2}) - 2\varphi_{hnf}\sigma_{bf}}{\varphi_\sigma + 2k_{bf} - (\varphi_{Cu}\sigma_{Cu} + \varphi_{UO_2}\sigma_{UO_2}) + \varphi_{hnf}\sigma_{bf}}$ where $\varphi_\sigma = \frac{\varphi_{Cu}\sigma_{Cu} + \varphi_{UO_2}\sigma_{UO_2}}{\varphi_{hnf}}$ |

**Table 2**
Thermophysical properties of base-fluid and various nanoparticles [58,60].

| Physical Properties | Blood | $UO_2$ | $Cu$ | $CuO$ | $Al_2O_3$ |
|---|---|---|---|---|---|
| $\rho$ (kg/m$^3$) | 1053 | 10970 | 8933 | 6320 | 3970 |
| $C_p$ (J/gK) | 3594 | 235 | 385 | 531.8 | 765 |
| $k$ (W/mK) | 0.492 | 8.68 | 400 | 76.5 | 40 |
| $\sigma$ (S/m) | 0.8 | 0.029 | $5.96\times10^7$ | $2.7\times10^{-8}$ | $35\times10^6$ |

$$F''' + \frac{2}{\wp_3}FF'' - \frac{F'^2}{\wp_3} + \frac{\wp_1}{\wp_2\wp_3}MF' - \frac{G^2}{\wp_3} - \frac{B}{\wp_3}\left(F' + \frac{\eta}{2}F''\right) = 0, \tag{10}$$

$$G'' - \frac{\wp_1}{\wp_2\wp_3}MG - \frac{B}{\wp_3}\left(G + \frac{\eta}{2}G'\right) - \frac{2}{\wp_3}(GF' - FG') = 0, \tag{11}$$

$$\frac{1}{Pr}\frac{\wp_4}{\wp_5}\theta'' + \frac{R^*}{\wp_5 Pr}\left\{3(1+\delta_1\theta)^2\delta_1\theta'^2 + (1+\delta_1\theta)^3\theta''\right\} - B\eta\theta' + 2F\theta' = 0, \tag{12}$$

$$\phi'' - \frac{\sigma_t Sc}{\wp_6}\phi(1+\delta_1\theta)^m \exp\left[\frac{-Et}{1+\delta_1\theta}\right] - \frac{Sc}{\wp_6}B\eta\phi + 2\frac{Sc}{\wp_6}F\phi' = 0, \tag{13}$$

with transformed boundary conditions as below

$$\begin{aligned} &F'(0) = \tilde{A}_1, \quad F(0) = Ws, \quad G(0) = 1, \quad \theta'(0) = -\mathbb{B}_1\{1-\theta(0)\}, \quad \phi(0) = 1, \quad at \quad \eta = 0, \\ &F'(1) = \tilde{A}_2, \quad G(1) = 0, \quad F(1) = 0, \quad \theta'(1) = \mathbb{B}_2\theta(1), \quad \phi(1) = 0, \quad at \quad \eta = 1. \end{aligned} \tag{14}$$

The dimensionless quantities in Eqs. (10)-(14) are defined as follows

$$\begin{aligned} &\wp_1 = \frac{\sigma_{hnf}}{\sigma_{bf}}, \quad \wp_2 = \frac{\rho_{hnf}}{\rho_{bf}}, \quad \wp_3 = \frac{\nu_{hnf}}{\nu_{bf}}, \quad \wp_4 = \frac{k_{hnf}}{k_{bf}}, \quad \wp_5 = \frac{(\rho Cp)_{hnf}}{\rho Cp_{bf}}, \\ &\wp_6 = \frac{D_{hnf}}{D_f}, \quad B = \frac{b}{\omega}, \quad Pr = \frac{(\rho Cp)_{bf}\nu_{bf}}{k_{bf}}, \quad R^* = \frac{-16\tilde{\sigma}}{3\tilde{k}k_{bf}}T_2^3, \quad T_w = \frac{T_1}{T_2} \\ &\sigma_t = \frac{k_r^2(1-bt)}{\omega}, \quad Sc = \frac{\nu_{bf}}{D_{bf}}, \quad Et = \frac{-\tilde{E}}{k^*T_2}, \quad \mathbb{B}_1 = \frac{h_1}{k_{bf}}\sqrt{\frac{\nu_{bf}(1-bt)}{\omega}}, \quad \tilde{A}_1 = \frac{a_1}{\omega}, \\ &M = B_0^2\frac{\sigma_{bf}}{\rho_{bf}\omega}, \quad \tilde{A}_2 = \frac{a_2}{\omega}, \quad Ws = \frac{-W_0}{2\sqrt{\omega\nu_{bf}}}, \quad \mathbb{B}_2 = \frac{h_2}{k_{bf}}\sqrt{\frac{\nu_{bf}(1-bt)}{\omega}}, \quad \delta_1 = T_w - 1, \end{aligned}$$

here $\wp_i$ are the dimensionless nanofluid parameters, $B$ the unsteady parameter, $Pr$ the Prandtl number, $R^*$ the radiation parameter, $T_w$ the temperature ratio, $\sigma_t$ the chemical reaction rate, $Sc$ the Schmidt number, $Et$ the activation energy parameter, $\mathbb{B}_1, \mathbb{B}_2$ are the Biot numbers, $\tilde{A}_1$ and $\tilde{A}_2$ the stretching parameters, $M$ the magnetic interaction parameter and $W_s$ the suction/injection parameter. The thermophysical properties of blood and nanoparticles $UO_2$, $Cu$, $CuO$ and $Al_2O_3$ at normal temperature of $25^o$ C are adopted from standard literature [58,60] in Table 2.

### 2.1. Skin friction

Due to presence of multiple nanoparticles in blood hybrid nanofluid, skin friction arises near artery walls. Let $\Upsilon_{wr}$ and $\Upsilon_{w\phi}$ denote radial and transversal skin friction on arterial walls depending on shear stresses in these directions, respectively. Shear stresses are defined as

$$\tilde{\Upsilon}_{wr} = [\mu_{nf}(u_z + u_\phi)]_{z=0}, \quad \tilde{\Upsilon}_{w\phi} = \left[\mu_{nf}\left(v_z + \frac{1}{r} + w_\phi\right)\right]_{z=0}. \tag{15}$$

Basic formulation of skin friction is then give as

$$C_f = \frac{\sqrt{\Upsilon_{wr}^2 + \Upsilon_{w\phi}^2}}{\rho_{bf}(\omega r)^2} \tag{16}$$

By using Eq. (9) and (15) in Eq. (16), following non-dimensional form of skin friction is obtained

$$Re^{\frac{1}{2}} C_f = \frac{\sqrt{F'(0)^2 + G'(0)^2}}{(1-\varphi)^{2.5}},$$

where $Re = \frac{\omega r^2}{\nu_{bf}}$ is a local unsteady Reynold number.

### 2.2. Nusselt number

In order to define rate of heat transfer through blood hybrid nanofluid flow, Nusselt number is utilized in this study. Nusselt number depends on thermal conductivity of the base fluid i.e. blood and an extra effect of thermal radiation which is also considered in current fluid model. General form of Nusselt number in this regard takes following defined form

$$Nu = \frac{rq_r}{k_{bf}(T_1 - T_2)} \tag{17}$$

applying Eq. (9) in Eq. (17), dimensionless heat transfer rate is obtained as

$$Re^{\frac{-1}{2}} Nu = -\wp_4 \theta'(0).$$

### 2.3. Sherwood number

Mass transfer rate through the arteries in hybrid nanofluid flow is defined with help of Sherwood number that depends on mass diffusivity and concentration of the base-fluid (blood). We consider mass transfer $\mathbb{Q}_m$ as

$$\mathbb{Q}_m = -D_{hnf}\left[\frac{\partial \phi}{\partial z}\right]_{z=0}. \tag{18}$$

Hence general Sherwood number is now defined as

$$Sh = \frac{r\mathbb{Q}_m}{D_{bf}(C_1 - C_2)}, \tag{19}$$

Eq. (19) after utilizing Eq. (18) and similarity transforms in Eq. (9) becomes

$$Re^{\frac{-1}{2}} Sh = -\wp_6 \phi'(0).$$

## 3. Optimal q-homotopy analysis method

The proposed methodology is a hybrid of q-HAM with Galerkin's and least square optimizers. In order to describe the proposed methodology on coupled non-linear systems, we first consider following system of four non linear ordinary differential equations

$$\mathbb{N}_i[\zeta_i(\eta)] = 0, \qquad \text{where } i = 1(1)4, \tag{20}$$

here $\mathbb{N}_i$ are the non-linear operators, $\eta$ is the independent variable and $\zeta_i$ are the unknown functions of $\eta$.

Algorithm of Optimal q-HAM is given in the following steps:

***Step 1: Homotopy construction***

Construct q-homotopy equations for Eq. (20) as

$$\mathbb{H}_i: \quad (1 - \ell \hat{q})\mathbb{L}_i[\varnothing_i(\eta;q) - \zeta_{i0}(\eta)] - qc_i\mathfrak{H}(\eta)(\mathbb{N}_i[\varnothing_i(\eta;q)]) = 0, \qquad \text{where } i = 1(1)4, \tag{21}$$

here $\ell \geq 1$, $q \in \left[0, \frac{1}{\ell}\right]$ is the new embedding parameter, $\mathfrak{H}(\eta)$ is a non-zero auxiliary function, $\mathbb{L}_i$ and $\mathbb{N}_i$ are the linear and non linear operators, respectively. The unknown functions are represented as $\varnothing_i(\eta; q)$ with initial guess $\zeta_{i0}(\eta)$ and convergence control parameters $c_i$.

It is noted that when $q = 0$ then Eq. (21) gives initial guess whereas for $q = \frac{1}{\ell}$ final solution is formed.

$$\varnothing_i(\eta; 0) = \zeta_{i0}(\eta), \quad \varnothing_i\left(\eta; \frac{1}{\ell}\right) = \zeta_i(\eta),$$

where in q-modified homotopy analysis method there is freedom of choice for selection of $\zeta_{i0}(\eta), \mathbb{L}_i$ and $\mathfrak{H}$.

***Step 2: Taylor's series expansion***

Expand the unknown functions $\varnothing_i(\eta; q)$ in form of Taylor series as

$$\varnothing_i(\eta; q) = \zeta_{i0}(\eta) + \sum_{j=1}^{\infty} \zeta_j(\eta) q^j, \qquad \text{where } i = 1(1)4, \tag{22}$$

and $\zeta_j$ are as follows

$$\zeta_j(\eta) = \frac{1}{j!} \frac{\partial^j \varnothing_i(\eta; q)}{\partial q^j}.$$

We substitute Eq. (22) in Eq. (21).

***Step 3: Initial guesses***

We assume that $\zeta_{i0}(\eta), \mathbb{L}$ and $\mathfrak{H}$ are chosen such that the series (22) converges at $q = \frac{1}{\ell}$ and the system becomes

$$\zeta_i(\eta) = \varnothing_i\left(\eta; \frac{1}{\ell}\right) = \zeta_{i0}(\eta) + \sum_{j=1}^{\infty} \zeta_j(\eta) \left(\frac{1}{\ell}\right)^j, \qquad \text{where } i = 1(1)4,$$

***Step 4: Deforming homotopy***

Differentiating Eq. (21) $j$ times with respect to q. We then set $q = 0$ and divide the final equations by $j!$ to obtain jth-order deformation equation as

$$\mathbb{L}[\zeta_j(\eta) - \varkappa_j u_{j-1}(\eta)] - c_i \mathfrak{H}(\eta) \mathfrak{R}_j(u_{j-1}(\eta)) = 0, \qquad \text{where } i = 1(1)4,$$

and $\mathfrak{R}_j$ are defined as

$$\mathfrak{R}_j(u_{j-1}(\eta)) = \frac{1}{(j-1)!} \left. \frac{\partial^{j-1}(\mathbb{N}[\varnothing_i(\eta; q)])}{\partial q^{j-1}} \right|_{q=0}$$

such that $\varkappa_j = 0$ if $j \leq 1$ and $\varkappa_j = \ell$ otherwise. It is to be emphasized here that the series solution obtained now will be dependent on unknown $c_i$'s i.e the series solution at jth-order will be of form $\tilde{\zeta}_i(\eta, c_i)$ where $i$ =1, 2, 3 and 4 for four set of equations.

***Step 5: Optimization***

Substitute the jth-order approximate solution $\tilde{\zeta}_i(\eta, c_i)$ in original Eq. (21) to obtain residual error as

$$\mathbb{R}(\eta, c_i) = \mathbb{N}(\tilde{\zeta}_i(\eta, c_i)), \qquad i = 1(1)4.$$

Various methods can be utilized to find optimal value of convergence control parameters, here we use least square and Galerkin's method.

In method of least square we write

$$\mathfrak{G}(\eta, c_i) = \int_c^d \mathbb{R}^2(\eta, c_1) d\eta.$$

In order to minimize $\mathfrak{G}(\eta, c_i)$ we use

$$\frac{\partial \mathfrak{G}}{\partial c_i} = 0, \quad i = 1, 2, 3, 4.$$

In case of Galerkin's method, following system is solved for optimized values of $c_i$'s

$$\int_c^d \mathbb{R} \frac{\partial \tilde{\zeta}_i}{\partial c_i} d\eta = 0, \quad i = 1, 2, 3, 4.$$

Approximate values of $c_i$'s are determined by choosing c and d from problem domain. By plugging back the obtained optimal parameters $c_i$'s in jth-order approximate solutions, more optimized solutions $\tilde{\zeta}_i(\eta)$ are obtained. The solution mechanism is further presented in block diagram form in Fig. 2.

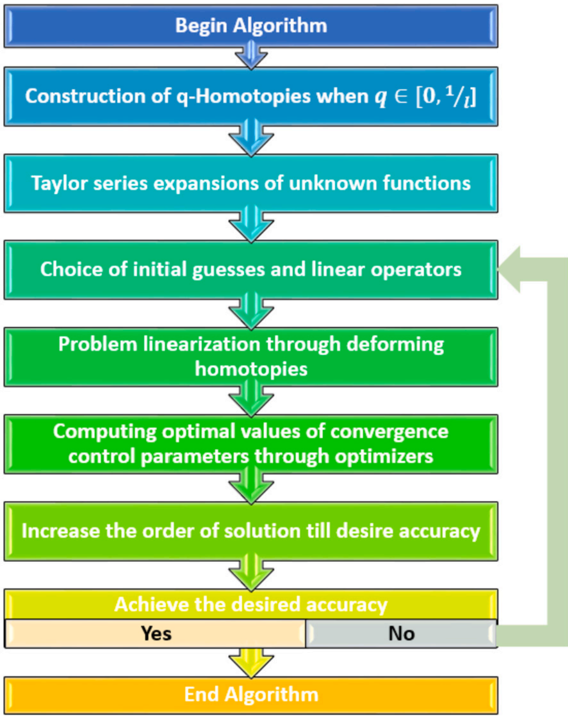


**Fig. 2.** Block diagram of optimal q-HAM.

## 4. Convergence analysis

In this section convergence of the solution obtained through optimal q-homotopy analysis method is discussed. For solution purpose of Eq. (10) along with boundary conditions in Eq. (14) we choose the linear operators as

$$\mathbb{L}_F = F'''(\eta), \quad \mathbb{L}_G = G''(\eta), \quad \mathbb{L}_\theta = \theta''(\eta), \quad \mathbb{L}_\phi = \phi''(\eta),$$

with initial guess

$$F(0) = Ws + \tilde{A}_1\eta + \frac{\tilde{A}_2 - \tilde{A}_1}{2}\eta^2, \quad G(0) = 1 - \eta$$
$$\theta(0) = \frac{\mathbb{B}_1\mathbb{B}_2 - \mathbb{B}_1 - \mathbb{B}_1\mathbb{B}_2\eta}{\mathbb{B}_2 - \mathbb{B}_1 + \mathbb{B}_1\mathbb{B}_2}, \qquad \phi(0) = 1 - \eta$$

We now use the optimal q-homotopy analysis method as described in Section 3, where subscript 1, 2, 3 and 4 will correspond to $F$, $G$, $\theta$, and $\phi$, respectively.

The optimal values of convergence control parameters are obtained as

$$c_F = -0.867619, \quad c_G = 1.27101, \quad c_\theta = -5.31998 \times 10^{-6}, \quad c_\phi = -1.43105.$$

Plot of averaged squared residual errors is also depicted in Fig. 3 till $35^{th}$ order of approximation. It is noted that with increase in order, squared residual errors decreased substantially. Moreover, squared residuals at various orders are also shown for $F(\eta)$, $G(\eta)$, $\theta(\eta)$, and $\phi(\eta)$ separately in Table 3.

## 5. Results and discussion

This section is focused on graphical analysis of blood hybrid nanofluid flow through arteries. Axial, radial and tangential profiles of velocity are studied for a comprehensive analysis of blood velocity. In Figs. 4(a), 4(b) and 5(a) it is observed that axial, radial and tangential velocity decreases with increasing volume fraction of uranium dioxide when copper volume fraction remains constant. Higher density of uranium dioxide in comparison with other nanoparticles (see Table 2) results in velocity drag which causes decrease in velocity with increasing $\varphi_{UO_2}$. Whereas, it is also worth mentioning that with addition of higher volume fraction of copper $\varphi_{Cu} = 0.38$, velocity profile decreases when compared with lower volume fraction i.e. $\varphi_{Cu} = 0.30$. In Fig. 5(b) and 5(c), temperature of blood hybrid nanofluid decreases while concentration increases with increase in $\varphi_{UO_2}$ when $\varphi_{Cu}$ is kept constant. As thermal conductivity of $UO_2$ is least as seen in Table 2, hence it causes temperature drop in the hybrid nanofluid. We further

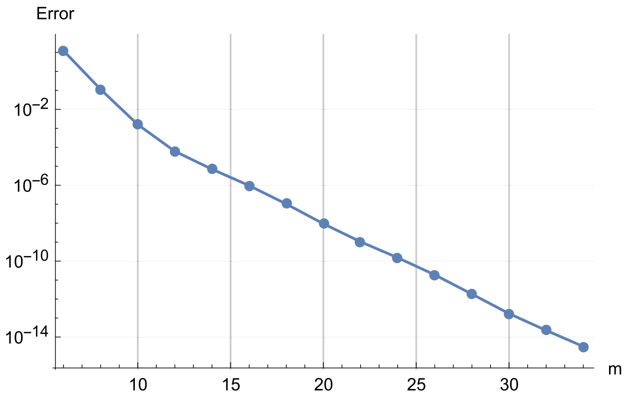


**Fig. 3.** Plot of squared residual error against order of approximation.

**Table 3**
Errors at various orders of approximations when $M = 1.3$, $B = 2.9$, $R^* = 0.2$, $Pr = 12$, $\delta_1 = 0.1$, $\sigma_t = 0.2$, $Sc = 1.3$, $Et = 0.8$, $\tilde{A}_1 = 1.1$, $\tilde{A}_2 = 1.2$, $Ws = 1.3$, $\mathbb{B}_1 = 0.9$, $\mathbb{B}_1 = 0.1$ and $\tilde{m} = 1.5$.

| Order of approx. | $F(\eta)$ | $G(\eta)$ | $\theta(\eta)$ | $\phi(\eta)$ |
|---|---|---|---|---|
| 4 | 0.0193619 | 0.0695947 | $1.789 \times 10^{3}$ | 0.259179 |
| 8 | 0.00030931 | 0.00012437 | 0.107269 | 0.00474783 |
| 16 | $6.28 \times 10^{-8}$ | $2.17 \times 10^{-9}$ | $1.96 \times 10^{-9}$ | $8.91 \times 10^{-7}$ |
| 18 | $7.20 \times 10^{-9}$ | $1.54 \times 10^{-10}$ | $2.66 \times 10^{-11}$ | $9.53 \times 10^{-8}$ |
| 22 | $9.35 \times 10^{-11}$ | $6.28 \times 10^{-13}$ | $4.21 \times 10^{-15}$ | $9.58 \times 10^{-10}$ |
| 28 | $1.32 \times 10^{-13}$ | $4.86 \times 10^{-16}$ | $9.19 \times 10^{-21}$ | $1.70 \times 10^{-12}$ |
| 32 | $1.64 \times 10^{-15}$ | $7.32 \times 10^{-18}$ | $1.44 \times 10^{-22}$ | $2.07 \times 10^{-14}$ |
| 34 | $1.82 \times 10^{-16}$ | $7.88 \times 10^{-19}$ | $3.18 \times 10^{-23}$ | $2.99 \times 10^{-15}$ |

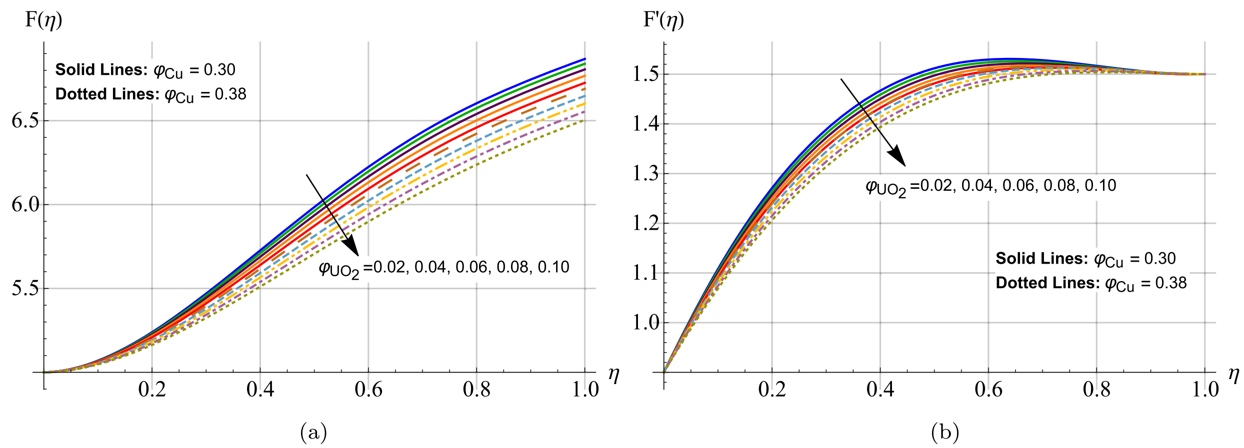


**Fig. 4.** Axial and radial velocity for different volume fractions of Cu.

check the temperature and concentration of blood flow when volume fraction of $Cu$ is increased. It is observed that for higher $\varphi_{Cu}$ temperature decreased and in contrast concentration of blood increased.

Skin friction, rate of heat transfer and mass transfer are shown in Figs. 6(a), 6(b) and 6(c) for increasing effect of $\varphi_{UO_2}$ on blood at x-axis. Skin friction is observed under influence of increasing magnetic parameter $M$, rate of heat transfer against increasing radiation parameter $R^*$ and mass transfer with increasing effect of activation energy parameter $Et$. In this sense most important parameters are considered to influence $C_f$, $Nu$ and $Sh$ for brief analysis of results. Firstly, we analyze how increase in $\varphi_{UO_2}$ on x-axis effects the skin friction, heat and mass transfer. As $\varphi_{UO_2}$ increases, skin friction and mass transfer of blood decreases whereas heat transfer increases. Secondly, effect of $M$, $R^*$ and $Et$ are noted. It is observed here that $M$ and $Et$ decreased the effect of higher $\varphi_{UO_2}$ while $R^*$ increases the effect on Nusselt number. And finally, volume fraction of copper is increased from 0.10 to 0.15. Skin friction and heat transfer are enhanced with addition of more copper in hybrid blood nanofluid and mass transfer rate is reduced with higher $\varphi_{Cu}$.

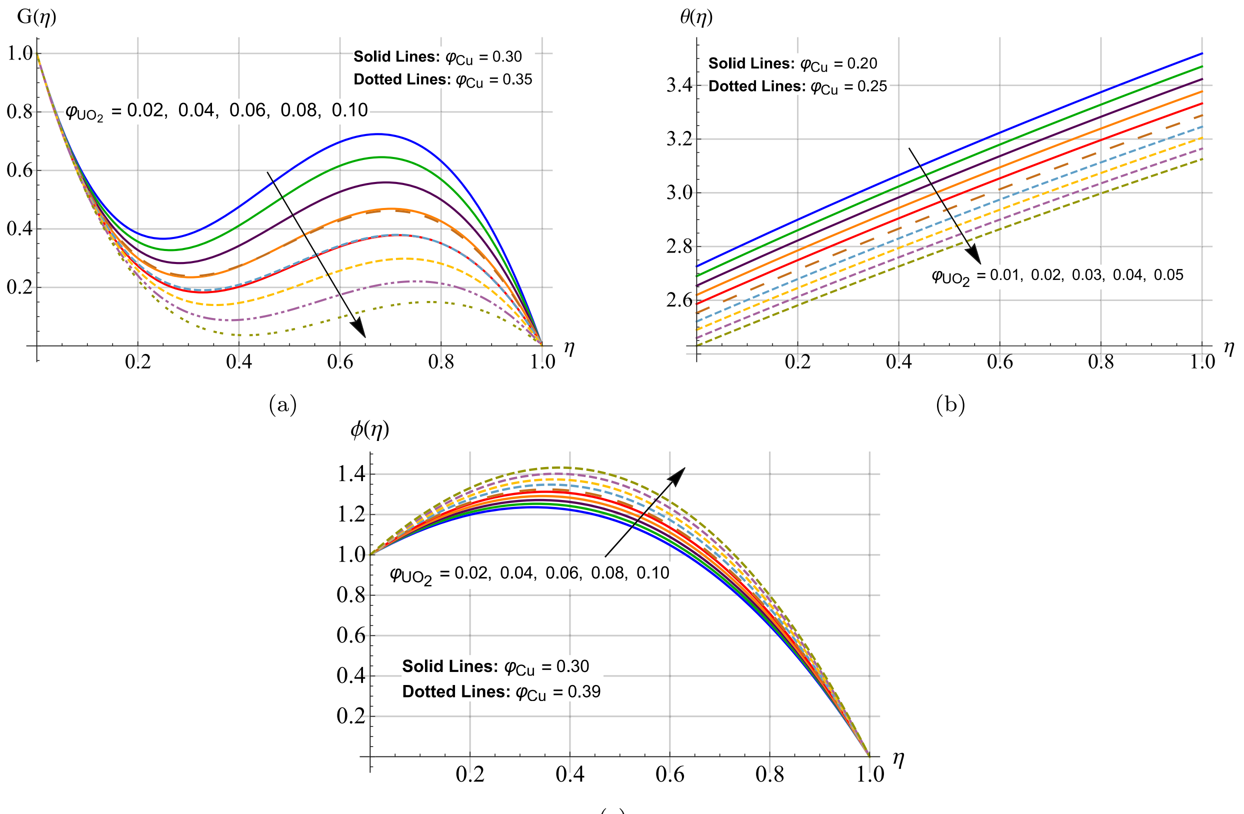


(a) (b) (c)

**Fig. 5.** Tangential velocity, temperature and concentration for different volume fractions of Cu.

**Table 4**
Percentage rate of change in physical quantities when $\varphi_{UO_2} = 0.01$.

| Property | $\varphi_{Cu} = 0.1$ | $\varphi_{Cu} = 0.15$ | Current | Experimental [22] |
|---|---|---|---|---|
| Skin friction | 6.01488 | 7.16676 | 19.15% | - |
| Heat transfer | 1.97435 | 2.2412 | 13.52% | 13.56% |
| Mass transfer | 1.3769 | 1.3269 | -3.63% | - |

Figs. 7(a), 7(b), 8(a), 8(b), 9(a) and 9(b) depict comparative effects of different nanoparticles, that is $Cu$, $CuO$ and $Al_2O_3$ on velocity, temperature, concentration, skin friction, mass and heat transfer of blood. $CuO$ shows least axial, radial and tangential velocity when compared with $CuO$ and $Al_2O_3$. Temperature of blood hybrid nanofluid is least in case of $Cu$ and highest in case of $Al_2O_3$. Moreover, skin friction of blood with arterial wall is maximum when $Cu$ nanoparticles are used while minimum skin friction is observed in case of $Al_2O_3$. Similarly, heat transfer rate through blood is most enhanced in case of $Cu$ nanoparticles and minimum when $Al_2O_3$ nanoparticles are added along with $UO_2$. As $Cu$ nanoparticles offers highest thermal conductivity in comparison with other nanoparticles hence it results in more heat transfer.

In order to sum up the analysis as a whole, the percentage change of skin friction, heat and mass transfer is calculated numerically and compared with experimental results in Table 4. It is observed that skin friction of blood with arterial walls was increased by 19.15% when copper volume fraction increased from 0.1 to 0.15. Similarly, rate of heat transfer through blood flow increased by 13.52% and mass transfer through arteries was decreased by 3.63%. Furthermore, the percentage increase of heat transfer numerically is in agreement with experimental results.

## 6. Conclusion

Main focus of current study is numerical and experimental analysis of hybrid blood-nanofluid. This study paves a way for medical sciences to characterize and optimize blood flow through arteries both theoretically and experimentally. A mathematical model is devised to depict rheological blood flow through arterial walls. Skin friction with walls that occur due to nanoparticles addition is also taken into account. Heat and mass transfer of blood through arterial walls is studied and compared with experimental data. In order to solve the modeled unsteady non-linear flow problem a new technique is employed that combines q-homotopy analysis method with Galerkin's and least square optimizers. The computed average squared residual errors justify the validity of proposed scheme.

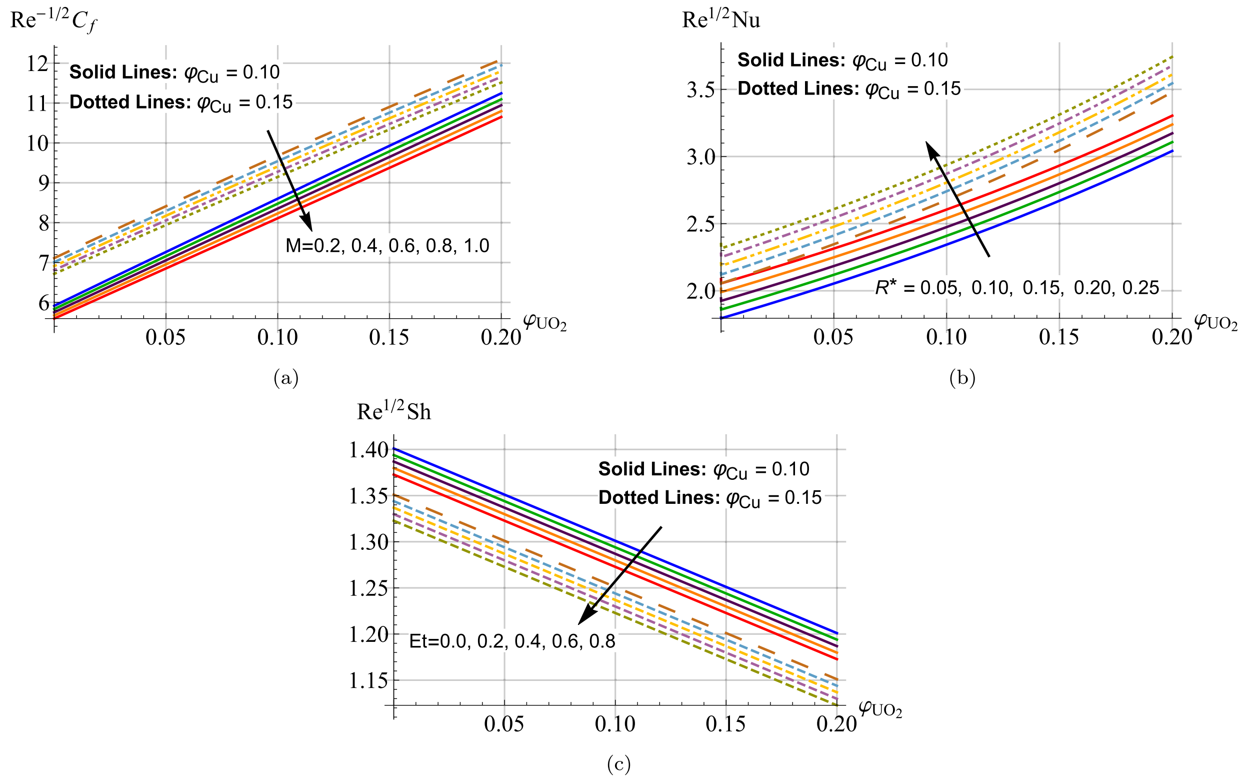


**Fig. 6.** Skin friction, heat transfer and mass transfer for different volume fractions of Cu.

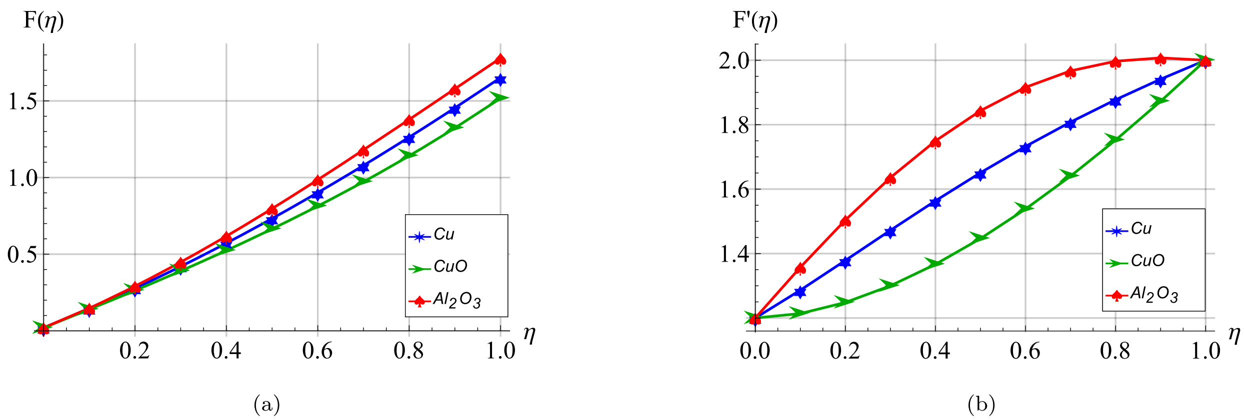


**Fig. 7.** Axial and radial velocity for different nanoparticles.

Velocity, temperature and concentration of blood flowing through arteries is computed for various values of volume fraction $\varphi_{Cu}$ with increasing volume fraction $\varphi_{UO_2}$. Different nanoparticles like copper, copper oxide and aluminum oxide are also compared with elevated levels of uranium dioxide volume fraction $\varphi_{UO_2}$ in blood. Increase in volume fraction of uranium dioxide $\varphi_{UO_2}$ decreases radial, axial, tangential velocity and temperature of blood whereas concentration increases in contrast. Moreover, aluminum oxide nanoparticles resulted in highest velocity (axial, radial) and blood hybrid nanofluid temperature when compared with copper and copper oxide. As higher volume fraction of copper was added, the effects of increasing $\varphi_{UO_2}$ on velocity (radial, axial and tangential) and temperature are reduced. On contrary, higher volume fraction of copper increased the effect of $\varphi_{UO_2}$ on blood concentration. Skin friction of blood with arterial walls and heat transfer through blood increased with higher levels of copper nanoparticles in hybrid nanofluid while mass transfer decreased in comparison. Highest tangential velocity, skin friction with arterial walls and heat transfer is caused by addition of copper nanoparticles with uranium dioxide in blood. With increase in volume fraction of copper nanoparticles in uranium effected blood, skin friction increased by 19.15%, heat transfer elevated by 13.52% and mass transfer was decreased by 3.63%. The findings of this study are consistent with experimental data as well. The current investigation can be further

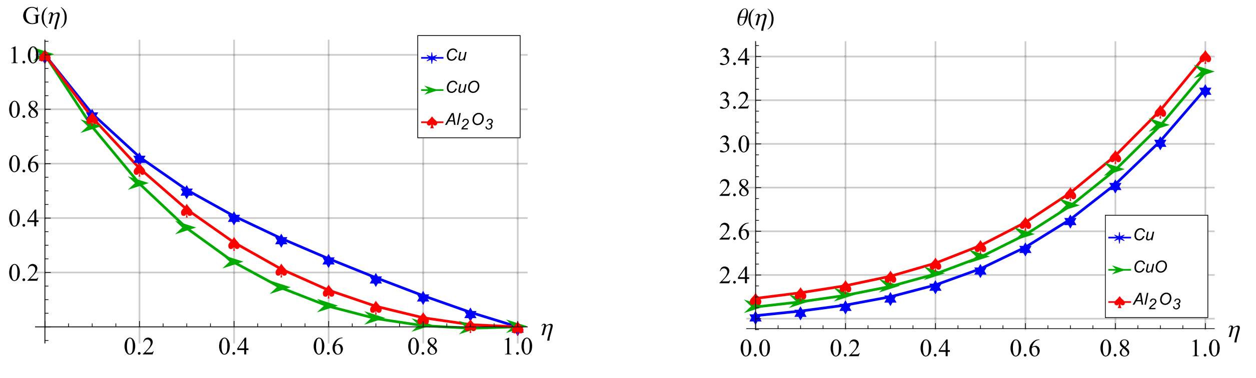


(a) (b)

**Fig. 8.** Tangential velocity and temperature for different nanoparticles.

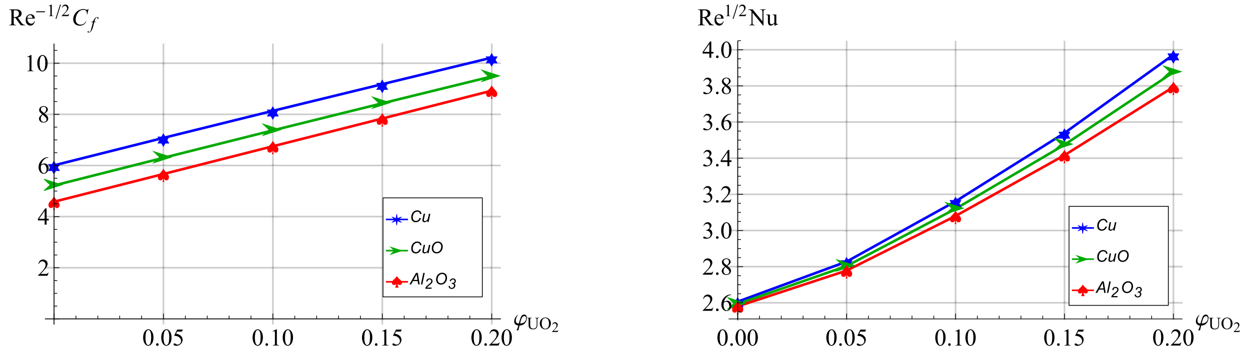


(a) (b)

**Fig. 9.** Skin friction and Nusselt number for different nanoparticles.

extended in future for oil based nanofluids in order to enhance the fuel efficiency and optimize the entropy generation by taking into account the heat and mass transfer effects.

### CRediT authorship contribution statement

Mubahir Qayyum: Conceived and designed the experiments; Analyzed and interpreted the data; Contributed reagents, materials, analysis tools or data; Wrote the paper.

Sidra Afzal: Conceived and designed the experiments; Performed the experiments; Analyzed and interpreted the data; Wrote the paper.

Syed Tauseef Saeed; Ali Akgül; Muhammad Bilal Riaz: Analyzed and interpreted the data; Contributed reagents, materials, analysis tools or data; Wrote the paper.

### Declaration of competing interest

The authors declare that they have no known competing financial interests or personal relationships that could have appeared to influence the work reported in this paper.

### Data availability

Data will be made available on request.

### References

[1] James Clerk Maxwell, Electricity and Magnetism, Electricity and Magnetism, vol. 2, Dover, New York, 1954.
[2] S.U.S. Choi, Jeffrey A. Eastman, Enhancing thermal conductivity of fluids with nanoparticles, No. ANL/MSD/CP-84938; CONF-951135-29, Argonne National Lab. (ANL), Argonne, IL, United States, oct 1995.
[3] Mustafa Turkyilmazoglu, Nanofluid flow and heat transfer due to a rotating disk, Comput. Fluids 94 (may 2014) 139–146.

[4] M. Sheikholeslami, M. Hatami, D.D. Ganji, Nanofluid flow and heat transfer in a rotating system in the presence of a magnetic field, J. Mol. Liq. 190 (feb 2014) 112–120.

[5] Gabriela Huminic, Angel Huminic, Entropy generation of nanofluid and hybrid nanofluid flow in thermal systems: a review, J. Mol. Liq. 302 (mar 2020) 112533.

[6] Jie Li, Clement Kleinstreuer, Thermal performance of nanofluid flow in microchannels, Int. J. Heat Fluid Flow 29 (4) (aug 2008) 1221–1232.

[7] Mohammad Ghalandari, Elaheh Mirzadeh Koohshahi, Fatemeh Mohamadian, Shahabbodin Shamshirband, Kwok Wing Chau, Numerical simulation of nanofluid flow inside a root canal, Eng. Appl. Comput. Fluid Mech. 13 (1) (jan 2019) 254–264.

[8] Mohsen Sheikholeslami, Davood Domiri Ganji, M. Younus Javed, R. Ellahi, Effect of thermal radiation on magnetohydrodynamics nanofluid flow and heat transfer by means of two phase model, J. Magn. Magn. Mater. 374 (jan 2015) 36–43.

[9] Ali Raza, Sami Ullah Khan, Kamel Al-Khaled, M. Ijaz Khan, Absar Ul Haq, Fakhirah Alotaibi, Abd Allah A. Mousa, Sumaira Qayyum, A fractional model for the kerosene oil and water-based Casson nanofluid with inclined magnetic force, Chem. Phys. Lett. 787 (jan 2022) 139277.

[10] Mubashir Qayyum, Omar Khan, Thabet Abdeljawad, Naveed Imran, Muhammad Sohail, Wael Al-Kouz, On behavioral response of 3d squeezing flow of nanofluids in a rotating channel, Complexity 2020 (oct 2020) 1–16.

[11] Khalid Abdulkhaliq M. Alharbi, Ibrahim B. Mansir, Kamel Al-Khaled, M. Ijaz Khan, Ali Raza, Sami Ullah Khan, Mohamed Ayadi, M.Y. Malik, Heat transfer enhancement for slip flow of single-walled and multi-walled carbon nanotubes due to linear inclined surface by using modified Prabhakar fractional approach, Arch. Appl. Mech. 92 (8) (jun 2022) 2455–2465.

[12] Kotha Gangadhar, Manda Aruna Kumari, Ali J. Chamkha, EMHD flow of radiative second-grade nanofluid over a riga plate due to convective heating: revised Buongiorno's nanofluid model, Arab. J. Sci. Eng. 47 (7) (aug 2021) 8093–8103.

[13] Fatema T. Zohra, Mohammed J. Uddin, Ahamd I.M. Ismail, Magnetohydrodynamic bio-nanoconvective naiver slip flow of micropolar fluid in a stretchable horizontal channel, Heat Transf. Asian Res. 48 (8) (aug 2019) 3636–3656.

[14] Gangadhar Kotha, Venkata Ramana Kolipaula, Munagala Venkata Subba Rao, Surekha Penki, Ali J. Chamkha, Internal heat generation on bioconvection of an MHD nanofluid flow due to gyrotactic microorganisms, Eur. Phys. J. Plus 135 (7) (jul 2020).

[15] Rabeeah Raza, Rahila Naz, Sara I. Abdelsalam, Microorganisms swimming through radiative sutterby nanofluid over stretchable cylinder: hydrodynamic effect, Numer. Methods Partial Differ. Equ. 39 (2) (sep 2022) 975–994.

[16] Sara I. Abdelsalam, Kh.S. Mekheimer, A.Z. Zaher, Dynamism of a hybrid Casson nanofluid with laser radiation and chemical reaction through sinusoidal channels, Waves Random Complex Media (apr 2022) 1–22.

[17] Muhammad Faizan, Farhan Ali, Karuppusamy Loganathan, Aurang Zaib, Ch Achi Reddy, Sara I. Abdelsalam, Entropy analysis of sutterby nanofluid flow over a riga sheet with gyrotactic microorganisms and Cattaneo–Christov double diffusion, Mathematics 10 (17) (sep 2022) 3157.

[18] K. Gangadhar, K. Bhanu Lakshmi, T. Kannan, Ali J. Chamkha, Bioconvective magnetized Oldroyd-b nanofluid flow in the presence of Joule heating with gyrotactic microorganisms, Waves Random Complex Media (mar 2022) 1–21.

[19] Kotha Gangadhar, R. Edukondala Nayak, M. Venkata Subba Rao, Ali J. Chamkha, Nonlinear radiations in chemically reactive Walter's b nanoliquid flow through a rotating cone, Proc. Inst. Mech. Eng., E J. Process Mech. Eng. (jun 2022) 095440892211059.

[20] Md. Jashim Uddin, O. Anwar Bég, Ahmad Izani Ismail, Radiative convective nanofluid flow past a stretching/shrinking sheet with slip effects, J. Thermophys. Heat Transf. 29 (3) (jul 2015) 513–523.

[21] O. Anwar Bég, Tasveer Bég, W.A. Khan, M.J. Uddin, Multiple slip effects on nanofluid dissipative flow in a converging/diverging channel: a numerical study, Heat Transf. 51 (1) (sep 2021) 1040–1061.

[22] S. Suresh, K.P. Venkitaraj, P. Selvakumar, M. Chandrasekar, Effect of Al2O3–Cu/water hybrid nanofluid in heat transfer, Exp. Therm. Fluid Sci. 38 (apr 2012) 54–60.

[23] Wajdi Alghamdi, Abdelaziz Alsubie, Poom Kumam, Anwar Saeed, Taza Gul, MHD hybrid nanofluid flow comprising the medication through a blood artery, Sci. Rep. 11 (1) (jun 2021).

[24] Saeed Dinarvand, Mohammadreza Nademi Rostami, Rassoul Dinarvand, Ioan Pop, Improvement of drug delivery micro-circulatory system with a novel pattern of CuO-Cu/blood hybrid nanofluid flow towards a porous stretching sheet, Int. J. Numer. Methods Heat Fluid Flow 29 (11) (nov 2019) 4408–4429.

[25] Iqra Shahzadi, S. Bilal, A significant role of permeability on blood flow for hybrid nanofluid through bifurcated stenosed artery: drug delivery application, Comput. Methods Programs Biomed. 187 (apr 2020) 105248.

[26] Sara I. Abdelsalam, Kh.S. Mekheimer, A.Z. Zaher, Alterations in blood stream by electroosmotic forces of hybrid nanofluid through diseased artery: aneurysmal/stenosed segment, Chin. J. Phys. 67 (oct 2020) 314–329.

[27] Hamidreza Shojaie Chahregh, Saeed Dinarvand, $TiO_2$-Ag/blood hybrid nanofluid flow through an artery with applications of drug delivery and blood circulation in the respiratory system, Int. J. Numer. Methods Heat Fluid Flow 30 (11) (feb 2020) 4775–4796.

[28] A.M. Alsharif, A.I. Abdellateef, Y.A. Elmaboud, S.I. Abdelsalam, Performance enhancement of a DC-operated micropump with electroosmosis in a hybrid nanofluid: fractional Cattaneo heat flux problem, Appl. Math. Mech. 43 (6) (jun 2022) 931–944.

[29] Faqir Shah, Sohail A. Khan, Kamel Al-Khaled, M. Ijaz Khan, Sami Ullah Khan, Nehad Ali Shah, Rifaqat Ali, Impact of entropy optimized Darcy-Forchheimer flow in $MnZnFe_2O_4$ and $NiZnFe_2O_4$ hybrid nanofluid towards a curved surface, Z. Angew. Math. Mech. 102 (3) (nov 2021).

[30] Awatif Alhowaity, Muhammad Bilal, Haneen Hamam, M.M. Alqarni, Kanit Mukdasai, Aatif Ali, Non-Fourier energy transmission in power-law hybrid nanofluid flow over a moving sheet, Sci. Rep. 12 (1) (jun 2022).

[31] Jinyuan Wang, Yi-Peng Xu, Raed Qahiti, M. Jafaryar, Mashhour A. Alazwari, Nidal H. Abu-Hamdeh, Alibek Issakhov, Mahmoud M. Selim, Simulation of hybrid nanofluid flow within a microchannel heat sink considering porous media analyzing CPU stability, J. Pet. Sci. Eng. 208 (jan 2022) 109734.

[32] J.K. Madhukesh, R. Naveen Kumar, R.J. Punith Gowda, B.C. Prasannakumara, G.K. Ramesh, M. Ijaz Khan, Sami Ullah Khan, Yu-Ming Chu, Numerical simulation of AA7072-AA7075/water-based hybrid nanofluid flow over a curved stretching sheet with Newtonian heating: a non-Fourier heat flux model approach, J. Mol. Liq. 335 (aug 2021) 116103.

[33] Naheeda Iftikhar, Hina Sadaf, Abdul Rehman, Consequences of gold nanoparticles of MHD blood flow in a wavy tube with wall properties, Waves Random Complex Media (jan 2022) 1–17.

[34] Rishu Gandhi, Bhupendra Kumar Sharma, Oluwole Daniel Makinde, Entropy analysis for MHD blood flow of hybrid nanoparticles (Au-$Al_2O_3$/blood) of different shapes through an irregular stenosed permeable walled artery under periodic body acceleration: hemodynamical applications, Z. Angew. Math. Mech. (oct 2022).

[35] Devendra Kumar, B. Satyanarayana, Rajesh Kumar, Sanjeev Kumar, Narendra Deo, Application of heat source and chemical reaction in MHD blood flow through permeable bifurcated arteries with inclined magnetic field in tumor treatments, Results Appl. Math. 10 (may 2021) 100151.

[36] Asma Khalid, Ilyas Khan, Arshad Khan, Sharidan Shafie, I. Tlili, Case study of MHD blood flow in a porous medium with CNTS and thermal analysis, Case Stud. Therm. Eng. 12 (sep 2018) 374–380.

[37] Mohammad Rashidi, Muhammad Bhatti, Munawwar Abbas, Mohamed Ali, Entropy generation on MHD blood flow of nanofluid due to peristaltic waves, Entropy 18 (4) (apr 2016) 117.

[38] Mohammad Rashidi, Zhigang Yang, Muhammad Bhatti, Munawwar Abbas, Heat and mass transfer analysis on MHD blood flow of Casson fluid model due to peristaltic wave, Therm. Sci. 22 (6 Part A) (2018) 2439–2448.

[39] Yinyin Wang, Ibrahim B. Mansir, Kamel Al-Khaled, Ali Raza, Sami Ullah Khan, M. Ijaz Khan, A. El-Sayed Ahmed, Thermal outcomes for blood-based carbon nanotubes (SWCNT and MWCNTs) with Newtonian heating by using new Prabhakar fractional derivative simulations, Case Stud. Therm. Eng. 32 (apr 2022) 101904.

[40] M.A. Elogail, Kh.S. Mekheimer, Modulated viscosity-dependent parameters for MHD blood flow in microvessels containing oxytactic microorganisms and nanoparticles, Symmetry 12 (12) (dec 2020) 2114.

[41] Anum Tanveer, Mair Khan, T. Salahuddin, M.Y. Malik, Farzana Khan, Theoretical investigation of peristaltic activity in MHD based blood flow of non-Newtonian material, Comput. Methods Programs Biomed. 187 (apr 2020) 105225.

[42] Kotha Gangadhar, E. Mary Victoria, Ali J. Chamkha, Hydrothermal features in the swirling flow of radiated graphene – $Fe_3O_4$ hybrid nanofluids through a rotating cylinder with exponential space-dependent heat generation, Waves Random Complex Media (jul 2022) 1–24.

[43] M.M. Bhatti, M. Ali Abbas, Simultaneous effects of slip and MHD on peristaltic blood flow of Jeffrey fluid model through a porous medium, Alex. Eng. J. 55 (2) (jun 2016) 1017–1023.

[44] Om Prakash, S.P. Singh, Devendra Kumar, Y.K. Dwivedi, A study of effects of heat source on MHD blood flow through bifurcated arteries, AIP Adv. 1 (4) (dec 2011) 042128.

[45] Bhavya Tripathi, Bhupendra Kumar Sharma, Two-phase analysis of blood flow through a stenosed artery with the effects of chemical reaction and radiation, Ric. Mat. (mar 2021).

[46] Ashis Kumar Roy, O. Anwar Bég, Mathematical modelling of unsteady solute dispersion in two-fluid (micropolar-Newtonian) blood flow with bulk reaction, Int. Commun. Heat Mass Transf. 122 (mar 2021) 105169.

[47] Rahmat Ellahi, Ahmed Zeeshan, Farooq Hussain, A. Asadollahi, Peristaltic blood flow of couple stress fluid suspended with nanoparticles under the influence of chemical reaction and activation energy, Symmetry 11 (2) (feb 2019) 276.

[48] H. Thameem Basha, R. Sivaraj, Numerical simulation of blood nanofluid flow over three different geometries by means of gyrotactic microorganisms: applications to the flow in a circulatory system, Proc. Inst. Mech. Eng., Part C, J. Mech. Eng. Sci. 235 (2) (aug 2020) 441–460.

[49] W.I.A. Okuyade, T.M. Abbey, M.E. Abbey, D.M. Abbey, A mathematical model of blood flow in merging veins under a magnetic resonance imaging influence, Eur. J. Math. Stat. 2 (3) (jun 2021) 1–7.

[50] Ghulam Rasool, Ting Zhang, Characteristics of chemical reaction and convective boundary conditions in Powell-Eyring nanofluid flow along a radiative riga plate, Heliyon 5 (4) (apr 2019) e01479.

[51] Zahir Shah, Poom Kumam, Wejdan Deebani, Radiative MHD Casson nanofluid flow with activation energy and chemical reaction over past nonlinearly stretching surface through entropy generation, Sci. Rep. 10 (1) (mar 2020).

[52] Noor Saeed Khan, Poom Kumam, Phatiphat Thounthong, Second law analysis with effects of arrhenius activation energy and binary chemical reaction on nanofluid flow, Sci. Rep. 10 (1) (jan 2020).

[53] Mubashir Qayyum, Hamid Khan, M. Tariq Rahim, Inayat Ullah, Analysis of unsteady axisymmetric squeezing fluid flow with slip and no-slip boundaries using OHAM, Math. Probl. Eng. 2015 (2015) 1–11.

[54] Omar Khan, Mubashir Qayyum, Hamid Khan, Murtaza Ali, Improved analysis for squeezing of Newtonian material between two circular plates, Adv. Mater. Sci. Eng. 2017 (2017) 1–9.

[55] Inayat Ullah, M.T. Rahim, Hamid Khan, Mubashir Qayyum, Analysis of various semi-numerical schemes for magnetohydrodynamic (MHD) squeezing fluid flow in porous medium, Propuls. Power Res. 8 (1) (mar 2019) 69–78.

[56] Svein Rosseland, Astrophysik, Springer, Berlin Heidelberg, 1931.

[57] Naveed Ahmed, Fitnat Saba, Umar Khan, Ilyas Khan, Tawfeeq Alkanhal, Imran Faisal, Syed Mohyud-Din, Spherical shaped ($Ag$ - $Fe_3O_4/H_2O$) hybrid nanofluid flow squeezed between two riga plates with nonlinear thermal radiation and chemical reaction effects, Energies 12 (1) (dec 2018) 76.

[58] M.M. Rashidi, S. Abelman, N. Freidooni Mehr, Entropy generation in steady MHD flow due to a rotating porous disk in a nanofluid, Int. J. Heat Mass Transf. 62 (jul 2013) 515–525.

[59] Masood Khan, Muhammad Azam, Unsteady heat and mass transfer mechanisms in MHD carreau nanofluid flow, J. Mol. Liq. 225 (jan 2017) 554–562.

[60] S. Srinivas, A. Vijayalakshmi, A. Subramanyam Reddy, Flow and heat transfer of gold-blood nanofluid in a porous channel with moving/stationary walls, J. Mech. 33 (3) (nov 2016) 395–404.